CORA Cork Open Research Archive
Cartlann Taighde Oscailte Chorcaí

Title	Quantum heat engine based on a spin-orbit- and Zeeman-coupled Bose-Einstein condensate
Authors	Li, Jing;Sherman, E. Ya;Ruschhaupt, Andreas
Publication date	2022-09-27
Original Citation	Li, J., Sherman, E. Y. and Ruschhaupt, A. (2022) 'Quantum heat engine based on a spin-orbit-and Zeeman-coupled Bose-Einstein condensate', Physical Review A, 106(3), L030201 (6pp). https://doi.org/10.1103/PhysRevA.106.L030201
Type of publication	Article (peer-reviewed);journal-article
Link to publisher's version	10.1103/PhysRevA.106.L030201
Rights	© 2022, American Physical Society. All rights reserved.
Download date	2026-11-16 14:37:16
Item downloaded from	https://hdl.handle.net/10468/17185

UCC
University College Cork, Ireland
Coláiste na hOllscoile Corcaigh

Letter

Quantum heat engine based on a spin-orbit- and Zeeman-coupled Bose-Einstein condensate

Jing Li [1,*] E. Ya Sherman [2,3,4] and Andreas Ruschhaupt [1]

[1]*Department of Physics, University College Cork, T12 H6T1 Cork, Ireland*
[2]*Departamento de Química-Física, UPV/EHU, Apartado 644, 48080 Bilbao, Spain*
[3]*IKERBASQUE, Basque Foundation for Science, 48011 Bilbao, Spain*
[4]*EHU Quantum Center, University of the Basque Country UPV/EHU, 48940 Leioa, Vizcaya, Spain*

(Received 21 June 2022; accepted 8 September 2022; published 27 September 2022)

We explore the potential of a spin-orbit-coupled Bose-Einstein condensate for thermodynamic cycles. For this purpose we propose a quantum heat engine based on a condensate with spin-orbit and Zeeman coupling as a working medium. The cooling and heating are simulated by contacts of the condensate with an external magnetized media and demagnetized media. We examine the condensate ground-state energy and its dependence on the strength of the synthetic spin-orbit and Zeeman couplings and interatomic interaction. Then we study the efficiency of the proposed engine. The cycle has a critical value of spin-orbit coupling related to the engine's maximum efficiency.

DOI: 10.1103/PhysRevA.106.L030201

Introduction. Quantum cycles are of much importance both for fundamental research and for applications in quantum-based technologies [1,2]. Quantum heat engines have been demonstrated recently on several quantum platforms, such as trapped ions [3,4], quantum dots [5], and optomechanical oscillators [6–9]. Well-developed techniques for experimental control make Bose-Einstein condensates (BECs) [10] a suitable system for a quantum working medium of a thermal machine [11–14].

Recently, a quantum Otto cycle was experimentally realized using a large quasispin system with individual cesium (Cs) atoms immersed in a quantum heat bath made of ultracold rubidium (Rb) atoms [15,16]. Several spin heat engines have been theoretically and experimentally implemented using a single-spin qubit [17], ultracold atoms [18], a single molecule [19], a nuclear magnetic resonance setup [20], and a single-electron spin coupled to a harmonic oscillator flywheel [21]. These examples have motivated our exploration of the spin-orbit-coupled BEC considered in this Letter.

Spin-orbit coupling (SOC) links a particle's spin to its motion, and artificially introduces chargelike physics into bosonic neutral atoms [22]. The experimental generation [23–26] of SOC is usually accompanied by a Zeeman field, which breaks various symmetries of the underlying system and induces interesting quantum phenomena, e.g., topological transport [27]. In addition, in BEC systems with SOC, studies on moving solitons [28–30], vortices [31], the stripe phase [32], and dipole oscillations [33] have been reported.

In this Letter, we propose a BEC with SOC as a working medium in a quantum Stirling cycle. The classic Stirling cycle is made of two isothermal strokes, connected by two isochores. The BEC is characterized by SOC, Zeeman splitting, a self-interaction, and is located in a quasi-one-dimensional vessel with a moving piston that changes its length. The external "cooling" and "heating" reservoirs are modeled by the interaction of the spin-$\frac{1}{2}$ BEC with external magnetized and demagnetized media. The expansion and compression works depend on the SOC and Zeeman coupling. Our main goal is to examine the condensate ground-state energy and its dependence on the strength of the synthetic spin-orbit, Zeeman couplings, interatomic interaction, and length of the vessel. For the semiquantitative analysis, perturbation theory is applied to understand the effects of SOC and Zeeman splitting. We further analyze several important parameters, e.g., the critical SOC strength for different self-interactions, and investigate how they affect the efficiency of the cycle.

Model of the heat engine: Working medium. We consider a quasi-one-dimensional BEC, extended along the x axis and tightly confined in the orthogonal directions. The mean-field energy functional of the system is then given by $E = \int_{-\infty}^{+\infty} \varepsilon dx$ with a spin-independent self-interaction of the Manakov's symmetry [34],

$$\varepsilon = \Psi^{\dagger}\mathcal{H}_0\Psi + \frac{g}{2}(|\psi_{\uparrow}|^2 + |\psi_{\downarrow}|^2)^2, \tag{1}$$

where $\Psi \equiv (\psi_{\uparrow}, \psi_{\downarrow})^{\mathrm{T}}$ (here, T stands for transposition) and the wave functions $\psi_{\uparrow}$ and $\psi_{\downarrow}$ are related to the two pseudospin components. The parameter g represents the strength of the atomic interaction which can be tuned by atomic s-wave scattering length using Feshbach resonance [35,36] with $g > 0$, $g < 0$, and $g = 0$ giving the repulsive, attractive, and no atomic interaction, respectively. The Hamiltonian $\mathcal{H}_0$ in Eq. (1) of the spin-$\frac{1}{2}$ BEC, trapped in an external potential $V(x)$, is given by

$$\mathcal{H}_0 = \frac{\hat{p}^2}{2m}\hat{\sigma}_0 + \frac{\alpha}{\hbar}\hat{p}\hat{\sigma}_x + \frac{\hbar}{2}\Delta\hat{\sigma}_z + V(x)\hat{\sigma}_0, \tag{2}$$

*Corresponding author: jli@ucc.ie

 ©2022 American Physical Society

with $\hat{p} = -i\hbar\partial_x$ being the momentum operator, $\hat{\sigma}_{x,z}$ being the Pauli matrices, and $\hat{\sigma}_0$ being the identity matrix. Here, α is the SOC constant and Δ is the Zeeman field. We choose a convenient length unit ξ, an energy unit $\hbar^2/(m\xi^2)$, and a time unit $m\xi^2/\hbar$, and express the following equations in the corresponding dimensionless variables. The coupled Gross-Pitaevskii equations are now given by

$$i\frac{\partial}{\partial t}\psi_\lambda = \left(-\frac{1}{2}\frac{\partial^2}{\partial x^2} + \frac{\Delta}{2} + g\,n(x) + V(x)\right)\psi_\lambda - i\alpha\frac{\partial}{\partial x}\psi_{\lambda'}, \tag{3}$$

where $(\lambda, \lambda') = (\uparrow, \downarrow)$ or $(\lambda, \lambda') = (\downarrow, \uparrow)$, and the density $n(x) = |\psi_\uparrow|^2 + |\psi_\downarrow|^2$. We fix the norm $N = \int_{-\infty}^{\infty} n(x)dx = 1$.

We consider a hard-wall potential $V(x)$ of the width w:

$$V(x) = 0 \quad (0 \leqslant x \leqslant w), \quad V(x) = \infty \quad (x < 0, x > w). \tag{4}$$

This potential is analogous to a piston in a thermodynamic cycle and allows one to define the work of the quantum cycle. The ground state Ψ of the BEC then depends on the width w, the detuning Δ, the interactions g, and the SOC α, i.e., $\Psi_{\alpha,g}(w, \Delta)$, and the corresponding ground-state energy of the BEC is then denoted as $E_{\alpha,g}(w, \Delta)$. We define the pressure which in a one-dimensional system coincides with a generalized force $P_{\alpha,g}(w, \Delta)$ as a measure of the energy $E_{\alpha,g}(w, \Delta)$ stored per length w:

$$P_{\alpha,g}(w, \Delta) \equiv -\frac{\partial E_{\alpha,g}(w, \Delta)}{\partial w}. \tag{5}$$

In the special case of $\Delta = 0$ and for the spin-independent self-interaction proportional to $n(x)$, the energy [37,38] is given by $E_{\alpha,g}(w, 0) = E_{0,g}(w, 0) - \alpha^2/2$ resulting in α-independent pressure $P_{\alpha,g}(w, 0)$. Notice that at both nonzero α and Δ, the system is characterized by a magnetostriction in the form $\mathcal{M}_{\alpha,g}(w, \Delta) = \partial P_{\alpha,g}(w, \Delta)/\partial\Delta$.

Model of the heat engine: Quantum Stirling cycle. We consider a quantum Stirling cycle keeping the interaction g and the SOC α fixed during the whole process. The key idea is that the external "cooling" and "heating" reservoirs are modeled by the interaction of the spin-$\frac{1}{2}$ BEC with external magnetized media [see Fig. 1(b), right] respectively demagnetized media [see Fig. 1(b), left]. This external (de)magnetized source leads to a random magnetic field in the condensate and because of the Zeeman effect this corresponds to a detuning of the condensate to Δ with some probability density distribution $p(\Delta)$. We assume that this external source brings the system to a stationary state with the condensate described by a density operator

$$\hat{\rho} = \int p(\Delta)|\Psi_{\alpha,g}(w, \Delta)\rangle\langle\Psi_{\alpha,g}(w, \Delta)|d\Delta. \tag{6}$$

The probability density distribution of the demagnetizing source $p_{\rm dm}(\Delta)$ is centered around $\langle\Delta\rangle_{\rm dm} \equiv \int \Delta\, p_{\rm dm}(\Delta)d\Delta = 0$ while the one of the magnetizing source $p_{\rm m}(\Delta)$ is centered around a positive value $\langle\Delta\rangle_{\rm m} > 0$. As an increase in Δ decreases the BEC energy [10] by an α-dependent amount, the demagnetization source plays the role of a "hot thermal bath" here and the magnetization source plays the role of a "cold thermal bath." In general there could exist a stationary external magnetic field leading to an additional detuning. Here, we neglect this possibility in order to simplify the notation.

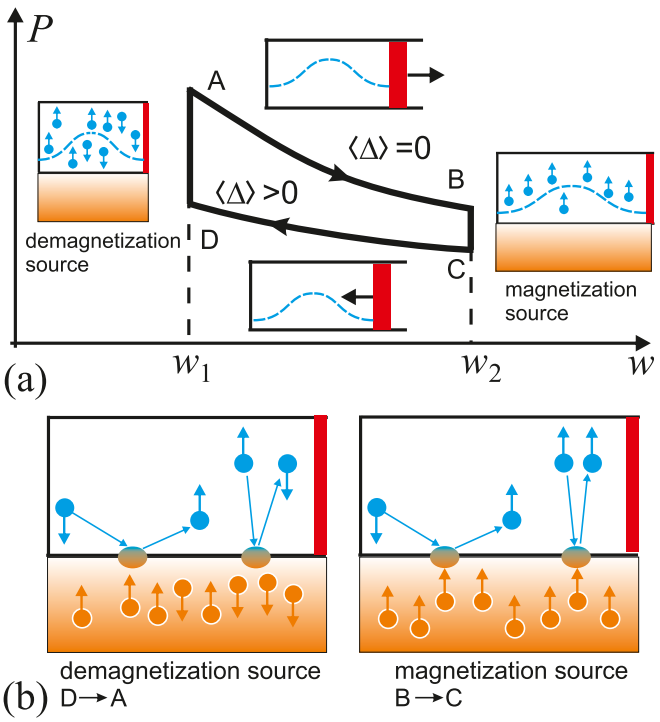


FIG. 1. (a) The schematic diagram of the quantum Stirling cycle based on the Zeeman and SOC. (b) Visualization of the demagnetization (left) and magnetization (right) processes with the external sources; the blue dots represent the BEC atoms and the orange dots represent the external source.

The realization of the Stirling cycle is described by a four-stroke protocol, illustrated in Fig. 1(a). We start at point A with the BEC being in contact with the demagnetization source, leading to an effective detuning centered around $\langle\Delta\rangle_{\rm dm} = 0$. The BEC state is given by Eq. (6) with $p(\Delta) = p_A(\Delta) \equiv p_{\rm dm}(\Delta)$.

Quantum "isothermal" expansion stroke $A \to B$. During this stroke, the working medium stays in contact with the external demagnetization source while the potential expands adiabatically from w_1 to w_2 without excitation in the BEC. The probability density distribution $p(\Delta)$ stays constant during this "isothermal" stroke, i.e., we have $p_A(\Delta) = p_B(\Delta) = p_{\rm dm}(\Delta)$ (effective detuning centered around $\langle\Delta\rangle_{\rm dm} = 0$). The average work done during this isothermal expansion stroke can be then calculated as [39] $\langle W_e\rangle = \int p_{\rm dm}(\Delta)[E_{\alpha,g}(w_1, \Delta) - E_{\alpha,g}(w_2, \Delta)]d\Delta$.

Quantum isochore cooling stroke $B \to C$. The contact with the demagnetization source is switched off and the working medium is brought into contact with the magnetization source while keeping w_2 constant. The probability distribution $p(\Delta)$ is changed to $p_C(\Delta) \equiv p_{\rm m}(\Delta)$, which corresponds to a "cooling" (as the total energy of the BEC is lowered). The average heat exchange in this stroke can be calculated as $\langle Q_c\rangle = \int[p_{\rm m}(\Delta) - p_{\rm dm}(\Delta)]E_{\alpha,g}(w_2, \Delta)d\Delta$.

Quantum "isothermal" compression stroke $C \to D$. During this stroke, the working medium stays in contact with the external magnetization source while the BEC compresses

adiabatically from potential width w_2 to w_1 without excitation in the BEC. The probability density distribution $p(\Delta)$ remains constant during this "isothermal" stroke, i.e., we have $p_D(\Delta) = p_C(\Delta) = p_{\rm m}(\Delta)$ leading to an effective detuning centered around $\langle\Delta\rangle_{\rm m} > 0$. The average work done during this isothermal compression is $\langle W_c\rangle = \int p_{\rm m}(\Delta)[E_{\alpha,g}(w_2,\Delta) - E_{\alpha,g}(w_1,\Delta)]d\Delta$.

Quantum isochore heating stroke $D \to A$. The contact with the magnetization source is switched off and the working medium is brought again into contact with the demagnetization source while keeping w_1 constant. The probability distribution $p(\Delta)$ is changed back to $p_A(\Delta) = p_{\rm dm}(\Delta)$, which corresponds to a "heating" (as the total energy of the BEC is increased). The average heat exchange in this stroke can be calculated as $\langle Q_h\rangle = \int[p_{\rm dm}(\Delta) - p_{\rm m}(\Delta)]E_{\alpha,g}(w_1,\Delta)d\Delta$.

To study this quantum cycle, it is important to examine and understand the dependence of the BEC ground-state energy on the different parameters. This will be done in the following.

Perturbation theory for the ground-state energy. The complex BEC system used in the thermodynamic cycle does not have an exact analytical solution. However, we can obtain analytical insight by considering perturbation theory of the ground-state energy $E_{\alpha,0}(w,\Delta)$ of the non-self-interacting BEC (i.e., $g = 0$) at small α (and nonzero Δ), as well as at small Δ (and nonzero α).

In the case of small $\alpha \ll 1/w$, the Hamiltonian in Eq. (1) can be written as $\mathcal{H}_0 = \mathcal{H}_{0,0} + \mathcal{H}_0'$, where $\mathcal{H}_0 = \hat{p}^2/2 + \Delta\hat{\sigma}_z/2 + V(x)$ and the perturbation term being $\mathcal{H}_0' = \alpha\hat{p}\hat{\sigma}_x$. The eigenstate basis of $\mathcal{H}_{0,0}$ is given by $\psi^{(0)}_{n,\downarrow}(x) = [0,\psi_n(x)]^{\rm T}$, $\psi^{(0)}_{n,\uparrow}(x) = [\psi_n(x),0]^{\rm T}$, where $\psi_n(x)$ are the eigenstates of the potential in Eq. (4). The first-order correction to the energy vanishes and the second-order correction becomes

$$\epsilon_2^{(0)} = -\sum_{n>1}\frac{\left|\langle\psi^{(0)}_{n,\uparrow}(x)|\mathcal{H}_0'|\psi^{(0)}_{0,\downarrow}(x)\rangle\right|^2}{(n^2-1)\pi^2/(2w^2)+\Delta}. \tag{7}$$

Thus, the ground-state energy $E_{\alpha,0}(w,\Delta)$ of the system up to second order in α is given by

$$E_{\alpha,0}(w,\Delta) \approx \frac{\pi^2}{2w^2} - \frac{\Delta}{2} - \frac{\pi^2\alpha^2}{w^2\Delta} + \frac{2\pi^2\alpha^2}{w^4\Delta^2}\zeta(w,\Delta), \tag{8}$$

where $\zeta(w,\Delta) \equiv \chi(w,\Delta)\cot[\chi(w,\Delta)/2]$ with $\chi(w,\Delta) \equiv \sqrt{\pi^2 - 2w^2\Delta}$. We can simplify Eq. (8) by approximating the expression up to first order in Δ:

$$E_{\alpha,0}(w,\Delta) \approx \frac{\pi^2}{2w^2} - \frac{\Delta}{2} - \frac{\alpha^2}{2} + \frac{\pi^2-6}{12\pi^2}\left(\frac{w}{\ell_{\rm sr}}\right)^2\Delta. \tag{9}$$

The first three terms on the right-hand side of Eq. (9) correspond to kinetic energy, Zeeman energy (at $\alpha = 0$), and SOC energy (at $\Delta = 0$). Here, we introduced the spin rotation length $\ell_{\rm sr} \equiv 1/\alpha$ with $w/\ell_{\rm sr} \ll 1$.

Alternatively, in the case of large $\alpha > 1/w$ and small detuning Δ, the Hamiltonian can be written as $\mathcal{H}_0 = \mathcal{H}_{0,1} + \mathcal{H}_1'$ where $\mathcal{H}_0 = \hat{p}^2/2 + \alpha\hat{p}\hat{\sigma}_x + V(x)$, and the perturbation term $\mathcal{H}_1' = \Delta\,\hat{\sigma}_z/2$. The unperturbed $\mathcal{H}_{0,1}$ has pairs of degenerate eigenstates $\psi_a^{(0)}$ and $\psi_b^{(0)}$ with the energy $E_{\alpha,0}(w,0)$:

$$\psi_a^{(0)}(x) = \psi_n(x)e^{-i\alpha x}\begin{pmatrix}1\\1\end{pmatrix}, \quad \psi_b^{(0)}(x) = \psi_n(x)e^{i\alpha x}\begin{pmatrix}1\\-1\end{pmatrix}. \tag{10}$$

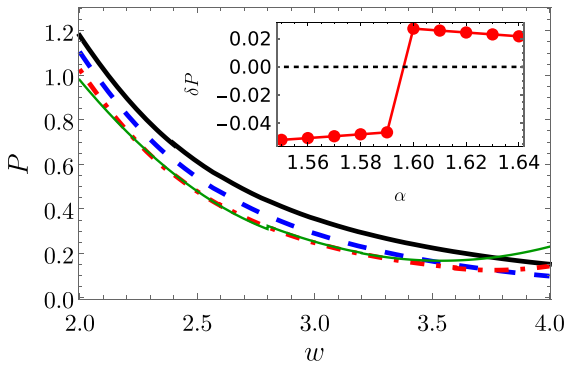


FIG. 2. Pressure $P_{\alpha,0}(w,\Delta)$ vs potential width w for the cases of $\Delta = 0$, $\alpha = 1.6$ (solid black, α independent), $\Delta = 1$, $\alpha = 1$ (dashed blue), $\Delta = 1$, $\alpha = 1.6$ (dotted-dashed red), and $\Delta = 1$, $\alpha = 1.75$ (solid green). Inset: The pressure difference between points C and B, $\delta P = P_{\alpha,0}(w_2,1) - P_{\alpha,0}(w_2,0)$.

Based on the perturbation theory for degenerate states and taking into account that the diagonal matrix elements of the perturbation $\Delta\langle\psi_i^{(0)}|\sigma_z|\psi_i^{(0)}\rangle/2 = 0$, we obtain at $w/\ell_{\rm sr} \gg 1$ the ground-state energy in the form

$$E_{\alpha,0}(w,\Delta) \approx \frac{\pi^2}{2w^2} - \frac{\alpha^2}{2} - \frac{\pi^2}{2}\frac{\ell_{\rm sr}/w}{|(w/\ell_{\rm sr})^2 - \pi^2|}\left|\sin\left(\frac{w}{\ell_{\rm sr}}\right)\right|\Delta. \tag{11}$$

When we look at the corresponding pressure following from Eq. (11), we can calculate approximately the pressure difference δP between the points B and C in the cycle (at w_2; see Fig. 1). The difference δP jumps from negative to positive at certain widths where $w_2/\ell_{\rm sr} \approx (n+1)\pi$ or $\alpha \approx (n+1)\pi/w_2$ with $n = 1, 2, 3, 4, \ldots$. In addition, there is always an α between two consecutive "jump points" where δP becomes zero. We will denote the first corresponding value of α, where the change of δP for negative to positive occurs, as the critical $\alpha_c(g,\Delta)$.

Energy and pressure. We examine now the exact numerical values of energy and pressure where we fix $w_1 = 2$ and $w_2 = 4$. The corresponding pressure is illustrated in Fig. 2 for a noninteracting BEC ($g = 0$). The shown pressure $P_{\alpha,0}(w_2,0)$ for $\Delta = 0$ is α independent, as discussed above. We can also see that the pressure $P_{\alpha,0}(w_2,1)$ is approximately equal to the pressure $P_{\alpha,0}(w_2,0)$ at $\alpha\, w_2 \approx 2\pi$, providing crossing between the red dashed-dotted line and black lines; this corresponds then to a critical $\alpha_c(0,1) \approx 1.6$. The corresponding δP is shown in detail in the inset; it can be seen that δP changes from negative to positive at $\alpha_c(0,1)$ as one expects it from the perturbation theory above.

In Fig. 3, the relations between the critical $\alpha_c(g,\Delta)$ and detuning Δ for different nonlinearities g are plotted. From the perturbation theory for $g = 0$ and for small Δ, one expects a value of $\alpha_c(g,\Delta) \approx 2\pi/w_2 \approx 1.57$. The figure shows that the exact α_c is increasing with increasing Δ for all cases of g. There is a competition between the SOC and Zeeman field, therefore, a larger detuning Δ requires automatically a larger α (and therefore a larger α_c) to have an effect. We also see that α_c is larger (smaller) for attractive $g = -1$ (repulsive $g = 1$) for all Δ. The heuristic reason is that there is a compression (expansion) of the wave function for $g < 0$ ($g > 0$) and,

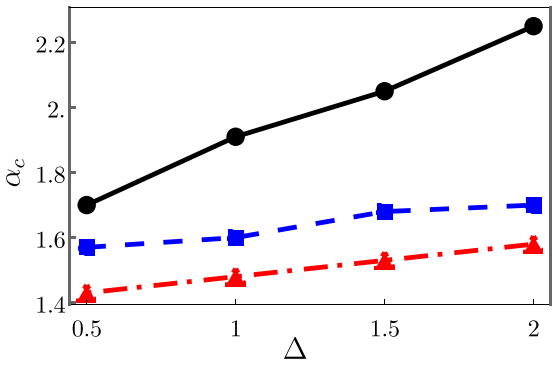


FIG. 3. Critical $\alpha_c(g, \Delta)$ vs detuning Δ for different nonlinearities: Attractive $g = -1$ (black solid line), noninteraction $g = 0$ (blue dashed line), and repulsive $g = 1$ (dotted-dashed red line).

therefore, a weaker (stronger) effect of SOC. This requires heuristically a larger (smaller) α (and therefore α_c) to show an effect.

Work, heat, and efficiency of the engine. Here, we are mainly interested in the properties of the cycle originating from the BEC and not in the details of the (de)magnetization source. Therefore, we assume that the probability density distributions $p_{\rm dm}$ and $p_{\rm m}$ are sharply peaked at $\langle\Delta\rangle_{\rm dm} = 0$ and $\langle\Delta\rangle_{\rm m} = \Delta_0 > 0$, respectively. Thus we approximate $p_{\rm dm}(\Delta) = \delta(\Delta)$ and $p_{\rm m}(\Delta) = \delta(\Delta - \Delta_0)$, where δ is the Dirac function. In this case, the black solid line and the blue dashed line in Fig. 2 present an example of the expansion and compression strokes of the cycle shown in the schematic Fig. 1. The work done during the "isothermal" expansion process in Fig. 1, $\langle W_e\rangle$, is then given by the energy differences $\langle W_e\rangle = E_{\alpha,g}(w_1, 0) - E_{\alpha,g}(w_2, 0)$. The cooling heat exchange from B to C $\langle Q_c\rangle$ through contact with the magnetization source, becomes $\langle Q_c\rangle = E_{\alpha,g}(w_2, \Delta_0) - E_{\alpha,g}(w_2, 0)$. The work $\langle W_c\rangle$ done during the compression stroke is then $\langle W_c\rangle = E_{\alpha,g}(w_2, \Delta_0) - E_{\alpha,g}(w_1, \Delta_0)$. The heat in the last stroke can be calculated by $\langle Q_h\rangle = E_{\alpha,g}(w_1, 0) - E_{\alpha,g}(w_1, \Delta_0)$. The total work then becomes

$$\mathcal{A} = \langle W_c\rangle + \langle W_e\rangle = \oint_{\rm ABCD} P_{\alpha,g}(w, \Delta_0)dw. \tag{12}$$

For small Δ_0,

$$\mathcal{A} = -\Delta_0 \int_{w_1}^{w_2} \mathcal{M}_{\alpha,g}(w, \Delta_0 \to 0)dw. \tag{13}$$

As defined above, at $\alpha = \alpha_c(g, \Delta_0)$, the pressures at w_2 for $\Delta = 0$ and $\Delta_0 > 0$ approximately coincide. If $\alpha > \alpha_c(g, \Delta_0)$, the pressure dependencies on a for $\Delta = 0$ and $\Delta_0 > 0$ cross at a certain width $\widetilde{w}$ with $w_1 < \widetilde{w} < w_2$ [see, for example, in Fig. 2, the case of $\alpha = 1.75$ (solid green line) where $\widetilde{w} \approx 3.8$]. In that case, the work at the interval $(\widetilde{w}, w_2)$ provides a negative contribution (work done on the system) to $\mathcal{A}$, while the contribution of the interval $(w_1, \widetilde{w})$, that is the work done by the system, is still positive. In the inset of Fig. 4(a), the total work $\mathcal{A}$ vs α is plotted. We see a maximum of $\mathcal{A}$ being close to $\alpha_c(g, \Delta_0)$. In the following, we restrict our analysis to the case $\alpha \leqslant \alpha_c(g, \Delta_0)$ (only work done by the system).

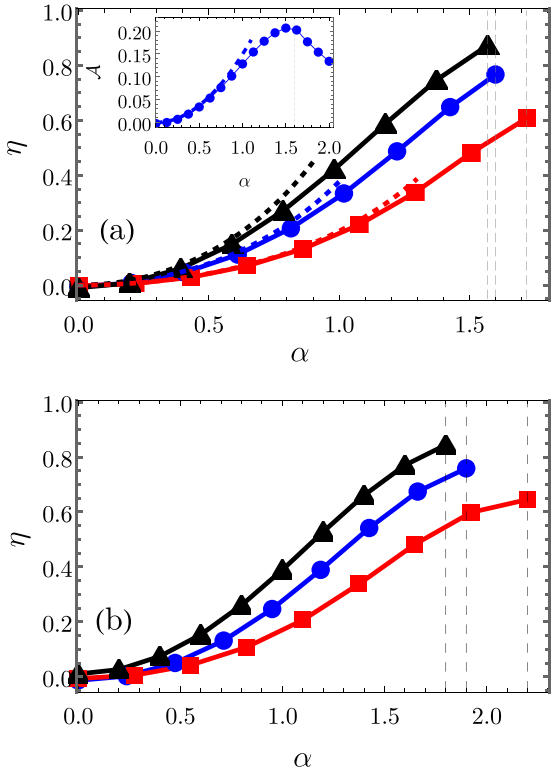


FIG. 4. Efficiency η vs α with $\Delta_0 = 0.5$ (solid black), $\Delta_0 = 1.0$ (solid blue), and $\Delta_0 = 2.0$ (solid red); the dotted vertical lines denote the critical SOC strength $\alpha_c(g, \Delta_0)$. (a) $g = 0$. Inset: Total work $\mathcal{A}$ vs α with $\Delta_0 = 1.0$; results based on perturbation theory in Eq. (15) (blue, red, and black dashed lines). (b) $g = -1$.

The efficiency of each quantum cycle is now defined as

$$\eta = \frac{\mathcal{A}}{\langle Q_h\rangle}. \tag{14}$$

At small $\alpha \ll 1/w$, where $\langle Q_h\rangle \approx \Delta_0/2$, we get $\eta \approx 2\mathcal{A}/\Delta_0$. Using Eq. (8), we approximate the total work $\mathcal{A}$ as

$$\mathcal{A} \approx \frac{\pi^2}{\Delta_0}\left[\left(\frac{1}{w_1^2} - \frac{1}{w_2^2}\right) + \frac{2}{\Delta_0}\left(\frac{\zeta(w_1, \Delta_0)}{w_1^4} - \frac{\zeta(w_2, \Delta_0)}{w_2^4}\right)\right]\alpha^2. \tag{15}$$

At $\Delta_0 \ll \pi^2/(2w_2^2)$, Eq. (15) yields for $\mathcal{A}$ and η,

$$\mathcal{A} = \frac{\pi^2 - 6}{12\pi^2}\Delta_0\left(w_2^2 - w_1^2\right)\alpha^2, \quad \eta = \frac{\pi^2 - 6}{6\pi^2}\left(w_2^2 - w_1^2\right)\alpha^2. \tag{16}$$

It is worth noticing that Eq. (16) has two limits with respect to the value of w_2. Let us define η_c as the efficiency at the critical α_c. First, Eq. (16) is applicable only at $\alpha\, w_2 < 2\pi$, thus limiting the critical η_c to the values of the order of 0.1. Second, for $g < 0$, the value of w_2 is limited to soliton width $4/|g|$ [40], thus η_c is limited correspondingly. [Notice that Eq. (16) is not directly applicable to $g \neq 0$ BEC.]

Figure 4 shows that the efficiency η grows as α increases. The approximate efficiency in Eq. (15) is a quadratic function of α, and this is in good agreement with the numerical results in Fig. 4(a) for the case $g = 0$. In the limit of $\Delta_0 \to 0$, the efficiency $\eta \sim \alpha^2$ [see Eq. (16)]. This limit case is also shown by the dashed pink line in Fig. 4(a). As one expects

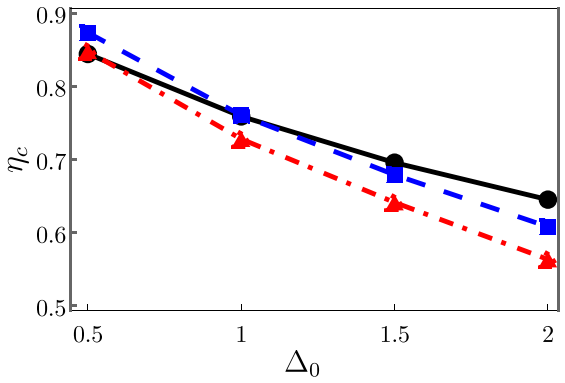


FIG. 5. Efficiency η_c at $\alpha_c(g, \Delta_0)$ vs Δ_0. Nonlinearities: Attractive $g = -1$ (black solid), noninteraction $g = 0$ (blue dashed), and repulsive $g = 1$ (dotted-dashed red). Values of $\alpha_c(g, \Delta_0)$ are the same as those in Fig. 3.

a maximum of the total work close to $\alpha_c(g, \Delta_0)$, one expects also that the efficiency reaches the maximum at α close to $\alpha_c(g, \Delta_0)$. The efficiency η_c at a critical α_c with respect to Δ_0 is shown in Fig. 5. The efficiency decreases with increasing Δ. This corresponds to Eq. (15) when $\alpha = \alpha_c \approx 2\pi/w_2$ for all three cases of g (see Fig. 3).

Discussion and conclusions. Here, we return to the physical units and discuss the possibility of the experimental realization of the present Stirling cycle. In the one-dimensional realization considered above, with the physical unit of length ξ, the resulting dimensionless coupling constant g can be estimated as $\sim 2\mathcal{N}a_{\rm at}\xi/s_{\rm p}$, where $s_{\rm p}$ is the condensate cross section, physically corresponding to the piston cross section. Here, $a_{\rm at}$ is the interatomic scattering length (typically of the order of $10a_B$, where a_B is the Bohr radius) dependent on the Feshbach resonance realization, and $\mathcal{N} \sim 10^3$ is the total number of atoms in the condensate [41]. A reasonable ξ for optical setups is of the order of 10 μm. Thus, the choice of w_1, w_2 of the order of 10 μm allows one to achieve stable well-controllable dimensionless α and Δ_0 of the order of unity [26], and thus explore the operational regimes of the Stirling cycle up to the critical values.

In summary, we have explored the potential of a spin-orbit-coupled Bose-Einstein condensate in a thermodynamic Stirling-like cycle. It takes advantage of both the noncommuting synthetic spin-orbit and Zeeman-like contributions. The "cooling" and "heating" is assumed to originate by an interaction with external magnetization and demagnetization media. We have examined the ground-state energy of the condensate and how the corresponding pressure depends on the system parameters. We have studied the efficiency of the corresponding engine in the dependence on the strength of these spin-related couplings. The cycle is characterized by a critical spin-orbit coupling, corresponding, essentially, to the maximum efficiency. The dependence of the efficiency on the spin-dependent coupling and nonlinear self-interaction paves the way to applications of these cycles. While we have concentrated here on the BEC-originated effects, it will be interesting to study in the future the details of external magnetization and demagnetization sources. In addition, one could examine if ideas of regeneration of the heat [42,43] could be also applied to the system of interest.

Acknowledgments. We are grateful to C. Whitty and D. Rea for commenting on the manuscript. J.L. and A.R. acknowledge that this publication has emanated from research supported in part by a Grant from Science Foundation Ireland under Grant number 19/FFP/6951 ("Shortcut-Enhanced Quantum Thermodynamics"). The work of E.S. is financially supported through Grants No. PGC2018-101355-B-I00 and No. PID2021-126273NB-I00 funded by MCIN/AEI/10.13039/501100011033 and by ERDF "A way of making Europe," and by the Basque Government through Grants No. IT986-16 and No. IT1470-22.

[1] J. Goold, M. Huber, A. Riera, L. del Rio, and P. Skrzypczyk, J. Phys. A: Math. Theor. **49**, 143001 (2016).
[2] S. Deffner and S. Campbell, *Quantum Thermodynamics* (Morgan & Claypool, San Rafael, CA, 2019).
[3] O. Abah, J. Roßnagel, G. Jacob, S. Deffner, F. Schmidt-Kaler, K. Singer, and E. Lutz, Phys. Rev. Lett. **109**, 203006 (2012).
[4] J. Roßnagel, S. T. Dawkins, K. N. Tolazzi, O. Abah, E. Lutz, F. Schmidt-Kaler, and K. Singer, Science **352**, 325 (2016).
[5] B. Sothmann, R. Sánchez, and A. N. Jordan, Nanotechnology **26**, 032001 (2015).
[6] K. Zhang, F. Bariani, and P. Meystre, Phys. Rev. Lett. **112**, 150602 (2014).
[7] C. Bergenfeldt, P. Samuelsson, B. Sothmann, C. Flindt, and M. Büttiker, Phys. Rev. Lett. **112**, 076803 (2014).
[8] C. Elouard, M. Richard, and A. Auffèves, New J. Phys. **17**, 055018 (2015).
[9] T. Hugel, N. B. Holland, A. Cattani, L. Moroder, M. Seitz, and H. E. Gaub, Science **296**, 1103 (2002).
[10] C. J. Pethick and H. Smith, *Bose-Einstein Condensation in Dilute Gases*, 2nd ed. (Cambridge University Press, Cambridge, UK, 2008), p. 316.
[11] C. Charalambous, M. A. Garcia-March, M. Mehboudi, and M. Lewenstein, New J. Phys. **21**, 083037 (2019).
[12] N. M. Myers, F. J. Peña, O. Negrete, P. Vargas, G. D. Chiara, and S. Deffner, New J. Phys. **24**, 025001 (2022).
[13] J. Li, T. Fogarty, S. Campbell, X. Chen, and T. Busch, New J. Phys. **20**, 015005 (2018).
[14] W. Niedenzu, I. Mazets, G. Kurizki, and F. Jendrzejewski, Quantum **3**, 155 (2019).
[15] F. Schmidt, D. Mayer, Q. Bouton, D. Adam, T. Lausch, J. Nettersheim, E. Tiemann, and A. Widera, Phys. Rev. Lett. **122**, 013401 (2019).
[16] Q. Bouton, S. Nettersheim, J. Burgardt, D. Adam, E. Lutz, and A. Widera, Nat. Commun. **12**, 2063 (2021).
[17] K. Ono, S. N. Shevchenko, T. Mori, S. Moriyama, and F. Nori, Phys. Rev. Lett. **125**, 166802 (2020).
[18] J.-P. Brantut, C. Grenier, J. Meineke, D. Stadler, S. Krinner, C. Kollath, T. Esslinger, and A. Georges, Science **342**, 713 (2013).
[19] W. Hübner, G. Lefkidis, C. D. Dong, D. Chaudhuri, L. Chotorlishvili, and J. Berakdar, Phys. Rev. B **90**, 024401 (2014).

[20] J. P. S. Peterson, T. B. Batalhão, M. Herrera, A. M. Souza, R. S. Sarthour, I. S. Oliveira, and R. M. Serra, Phys. Rev. Lett. **123**, 240601 (2019).
[21] D. von Lindenfels, O. Gräb, C. T. Schmiegelow, V. Kaushal, J. Schulz, M. T. Mitchison, J. Goold, F. Schmidt-Kaler, and U. G. Poschinger, Phys. Rev. Lett. **123**, 080602 (2019).
[22] Y. Zhang, M. E. Mossman, T. Busch, P. Engels, and C. Zhang, Front. Phys. **11**, 118103 (2016).
[23] Y.-J. Lin, K. Jiménez-García, and I. B. Spielman, Nature (London) **471**, 83 (2011).
[24] C. Wang, C. Gao, C.-M. Jian, and H. Zhai, Phys. Rev. Lett. **105**, 160403 (2010).
[25] T.-L. Ho and S. Zhang, Phys. Rev. Lett. **107**, 150403 (2011).
[26] D. L. Campbell, G. Juzeliūnas, and I. B. Spielman, Phys. Rev. A **84**, 025602 (2011).
[27] D. Xiao, M.-C. Chang, and Q. Niu, Rev. Mod. Phys. **82**, 1959 (2010).
[28] V. Achilleos, D. J. Frantzeskakis, P. G. Kevrekidis, and D. E. Pelinovsky, Phys. Rev. Lett. **110**, 264101 (2013).
[29] Y. Xu, Y. Zhang, and B. Wu, Phys. Rev. A **87**, 013614 (2013).
[30] Y. V. Kartashov and V. V. Konotop, Phys. Rev. Lett. **118**, 190401 (2017).
[31] J. Radić, T. A. Sedrakyan, I. B. Spielman, and V. Galitski, Phys. Rev. A **84**, 063604 (2011).
[32] S. Sinha, R. Nath, and L. Santos, Phys. Rev. Lett. **107**, 270401 (2011).
[33] J.-Y. Zhang, S.-C. Ji, Z. Chen, L. Zhang, Z.-D. Du, B. Yan, G.-S. Pan, B. Zhao, Y.-J. Deng, H. Zhai, S. Chen, and J.-W. Pan, Phys. Rev. Lett. **109**, 115301 (2012).
[34] S. V. Manakov, Sov. Phys. JETP **65**, 248 (1974).
[35] E. Tiesinga, A. J. Moerdijk, B. J. Verhaar, and H. T. C. Stoof, Phys. Rev. A **46**, R1167 (1992).
[36] P. Courteille, R. S. Freeland, D. J. Heinzen, F. A. van Abeelen, and B. J. Verhaar, Phys. Rev. Lett. **81**, 69 (1998).
[37] D. Sánchez and L. Serra, Phys. Rev. B **74**, 153313 (2006).
[38] I. V. Tokatly and E. Y. Sherman, Ann. Phys. **325**, 1104 (2010).
[39] P. Talkner, E. Lutz, and P. Hänggi, Phys. Rev. E **75**, 050102(R) (2007).
[40] C. Sulem and P.-L. Sulem, *The Nonlinear Schrödinger Equation: Self-Focusing and Wave Collapse*, Applied Mathematical Sciences Vol. 139 (Springer, Berlin, 1999).
[41] K. Henderson, C. Ryu, C. MacCormick, and M. G. Boshier, New J. Phys. **11**, 043030 (2009).
[42] X.-L. Huang, X.-Y. Niu, X.-M. Xiu, and X.-X. Yi, Eur. Phys. J. D **68**, 32 (2014).
[43] Y. Yin, L. Chen, and F. Wu, Eur. Phys. J. Plus **132**, 45 (2017).